Self-Complementary Nonlinear Optical-Phores Targeted to Halogen Bond-Driven Self-Assembly of Electro-Optic Materials

11 AUTHORS, INCLUDING:

Alessandra Forni
Italian National Research Council
109 PUBLICATIONS **1,502** CITATIONS

SEE PROFILE

Franck Meyer
Université Libre de Bruxelles
81 PUBLICATIONS **2,057** CITATIONS

SEE PROFILE

Giuseppe Resnati
Politecnico di Milano
334 PUBLICATIONS **10,171** CITATIONS

SEE PROFILE

Elisa Tordin
Johannes Kepler University Linz
35 PUBLICATIONS **267** CITATIONS

SEE PROFILE

Self-Complementary Nonlinear Optical-Phores Targeted to Halogen Bond-Driven Self-Assembly of Electro-Optic Materials

Published as part of the Crystal Growth & Design virtual special issue on Halogen Bonding in Crystal Engineering: Fundamentals and Applications

Elena Cariati,*,[†] Gabriella Cavallo,[‡] Alessandra Forni,*,[§] Gyu Leem,[#] Pierangelo Metrangolo,*,[‡,#] Franck Meyer,[#] Tullio Pilati,[§] Giuseppe Resnati,*,[‡,§,#] Stefania Righetto,[†] Giancarlo Terraneo,[‡,#] and Elisa Tordin[†]

[†]DCIMA and INSTM UdR Milano, University of Milan, via Venezian 21, I-20133 Milan, Italy
[‡]Center for Nano Science and Technology@Polimi, Istituto Italiano di Tecnologia, via Pascoli 70/3, I-20133 Milan, Italy
[§]ISTM-CNR, Università degli Studi di Milano, via Golgi 19, I-20133 Milan, Italy
[#]NFMLab, DCMIC "Giulio Natta", Politecnico di Milano, via Mancinelli 7, I-20131 Milan, Italy

Ⓢ Supporting Information

ABSTRACT: Three new push—pull molecules having either pyridyl or *N*,*N*-dimethylanilino groups as electron-donor moieties and the *p*-iodo-tetrafluorophenyl ring as an electron-acceptor group have been synthesized and their single crystal X-ray structures are reported. Halogen bonding drives the self-assembly of these molecules in the solid state giving rise to head-to-tail halogen-bonded infinite polar chains which crystallize in an antiparallel arrangement. The three new nonlinear optical (NLO)-phores synthesized show high hyperpolarizabilities at the molecular level in solution. Rationalization of the obtained NLO measurements is supported by molecular modeling calculations.
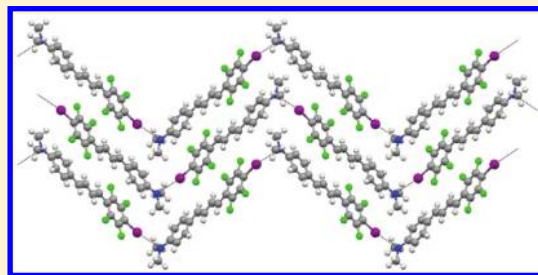
■ INTRODUCTION

Self-assembly of molecular modules through hydrogen bonding (HB) is a widely used technique for achieving nanoscale organization in supramolecular chemistry and materials science.[1] However, HB has rarely been used to fabricate electro-optically active two-dimensional (2D) thin films.[2] On the other hand, it has been demonstrated that strategies based on HB-driven self-assembly may have a great potential for the design of transparent organic films with very high electro-optical responses.[3] In particular, HB is effective for fabricating self-assembled nanoscopically acentric films showing very large optical nonlinearities (NLO).[4]

A full utilization of the so-called bottom-up approach to functional materials requires a continuous search for new and effective noncovalent interactions for assembling supramolecular structures possessing pre-established functions. It has been demonstrated how halogen bonding (XB),[5] namely, the noncovalent interactions involving halogen atoms as acceptors of electron density, is a new item in the supramolecular toolbox for assembling molecules into supramolecules. XB nicely complements HB and extends the range of supramolecular synthons for the preparation of self-assembled organic materials.[5g] The great potential of XB in the design of new and high-value functional materials, as well as in other fields wherein control of supramolecular organization plays a key-role, is now clearly emerging.[6] In

order to extend the use of XB in the design of organic materials for nonlinear optical (NLO) and optoelectronic applications,[7] we report here the synthesis and characterization of a new family of self-complementary tectons targeted to XB-based self-assembly of NLO-active materials. The molecular structures of these tectons are push—pull systems based on either pyridyl or *N*,*N*-dimethylanilino groups as electron-donor moieties and the *p*-iodo-tetrafluorophenyl ring as an electron-acceptor group, connected through different conjugated spacers in order to tune NLO responses. At the same time, the two units act as halogen-bonding acceptor and donor sites, respectively, in the XB-scheme, in analogy with the hydrogen bonding one. Thanks to the self-complementarity of the binding sites at the molecular ends, these tectons self-organize in the bulk crystalline state giving rise to head-to-tail halogen-bonded infinite chains. In this paper, the second-order NLO properties of three members of this new class of XB-based NLO-phores were evaluated at the molecular level by the solution-phase electric field induced second-harmonic (EFISH)[8−10] generation method. Rationalization of the obtained NLO measurements is supported by molecular modeling calculations.

Table 1. Crystallographic Data for Crystals 1−3

structure	1	2	3
chemical formula (moiety)	$C_{18}H_{14}F_4IN$	$C_{24}H_{18}F_4IN$	$C_{25}H_{23}F_4IN_2$
formula weight	447.20	523.29	554.35
temperature [K]	293(2)	297(2)	297(2)
radiation, wavelength [Å]	MoKα, 0.71073	MoKα, 0.71073	MoKα, 0.71073
crystal system	monoclinic	monoclinic	monoclinic
space group	$P2_1/n$	$P2_1/n$	$P2_1/c$
a [Å]	6.3296(8)	6.257(4)	8.7259(3)
b [Å]	23.958(3)	29.581(16)	14.6235(7)
c [Å]	10.9416(12)	10.904(6)	18.1206(7)
α [°]	90.00	90.00	90.00
β [°]	93.289(12)	96.02(2)	92.058(3)
γ [°]	90.00	90.00	90.00
cell volume [Å^3]	1656.5(3)	2007(2)	2310.76(16)
ρ_{calc} [g cm^{-3}]	1.793	1.732	1.593
Z	4	4	4
dimension [mm^3]	0.025 × 0.12 × 0.28	0.001 × 0.1 × 0.22	0.01 × 0.02 × 0.02
μ(MoKα) [mm^{-1}]	1.973	1.643	1.433
T_{min}, T_{max}	0.837276, 1.000000	0.48304, 1.000	0.6376, 0.7454
$F(000)$	872	1032	1104
crystal color shape	orange-yellow plate	yellow "bidimensional" plate	purple block
θ_{max} [°]	27.53	20.11	25.00
data collected	34131	7601	23034
unique data	3817	1885	4072
R_{int}	0.0308	0.1430	0.0896
no. obs. data $I_o > 2\sigma(I_o)$]	3188	1022	2316
no. parameters	273	272	290
no. restraints	64	162	
R_{all}	0.0390	0.1416	0.1088
R_{obs}	0.0316	0.0587	0.0425
wR_{all}	0.0890	0.1538	0.0956
wR_{obs}	0.0835	0.1189	0.0760
goodness-of-fit on F^2	1.054	0.991	1.012
$\Delta\rho_{min,max}$ [e Å^{-3}]	−0.350, 1.100	−0.545, 0.663	−0.335, 0.391
CCDC	299600	299599	843104

■ EXPERIMENTAL SECTION

Materials and Methods. All reagents were purchased from commercial suppliers (Apollo and Sigma Aldrich) and used without further purification. IR spectra were obtained using a Nicolet Nexus FTIR spectrometer equipped with a U-ATR device. The values were given in wave numbers and were rounded to 1 cm^{-1} upon automatic assignment. Melting points were determined by differential scanning calorimetry (DSC) analysis using a Mettler Toledo DSC 823e. Compounds **1−3** were synthesized following classical procedures of organic chemistry, as detailed in the Supporting Information. For the preparation of single crystals, compounds **1−3** were dissolved in chloroform in a vial of clear borosilicate glass. The open vials were closed in cylindrical wide-mouth jars containing paraffin oil. The solvent was allowed to evaporate at room temperature for a few days until the formation of crystals.

X-ray Structure Analyses. Single crystals of **1−3** suitable for X-ray analysis were mounted on a glass rod and analyzed. X-ray measurements were carried out on a Bruker SMART-APEX CCDC area detector diffractometer using graphite monochromatized Mo−K$_\alpha$ radiation (λ = 0.71073 Å) with a fine-focus sealed tube. CCDC nos.

299600, 299599, and 843104 contain the supplementary crystallographic data for **1**, **2**, and **3**, respectively. These data can be obtained free of charge from the Cambridge Crystallographic Data Centre via www.ccdc.cam.ac.uk/data_request/cif. Experimental details for the structure determination of **1−3** are given in Table 1.

EFISH Measurements. $\mu\beta_\lambda$ values have been directly obtained from EFISH measurements considering negligible the γ_0 contribution to γ_{EFISH} in eq 1.

$$\gamma_{EFISH} = \frac{\mu\beta_\lambda}{5kT} + \gamma_0(-2\omega; \omega, \omega, 0) \qquad (1)$$

where $(\mu\beta_\lambda)/(5kT)$ is the dipolar orientational contribution, β_λ is the projection along the dipole moment axis of the vectorial component β_{VEC} of the quadratic hyperpolarizability tensor, μ is the static dipole moment, ω is the fundamental wavelength of the incident photon, and $\gamma_0(-2\omega; \omega, \omega, 0)$, a third-order term at frequency ω of the incident light, is the cubic electronic contribution to γ_{EFISH}.

Measurements were carried out in CHCl$_3$ and DMF solutions working at a nonresonant incident wavelength of 1.907 μm, using a Q-switched, mode-locked Nd^{3+}:YAG laser, equipped with a Raman

Scheme 1. Chemical Formulas of the Self-Complementary XB-Based Tectons 1−5
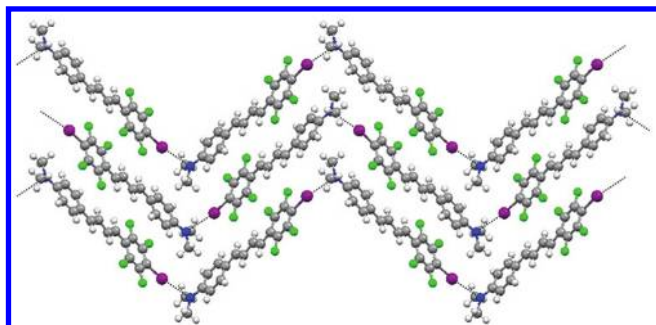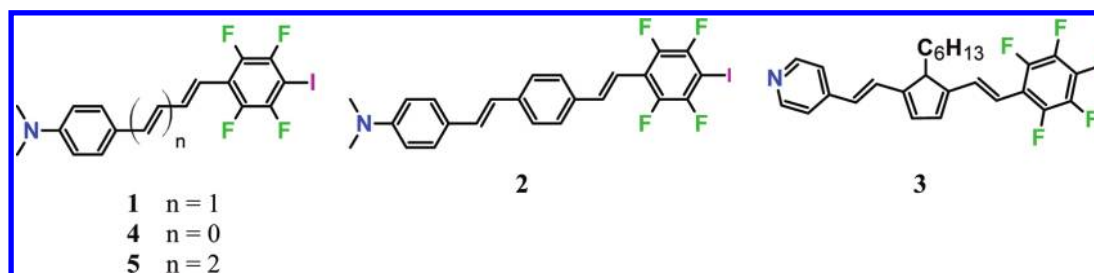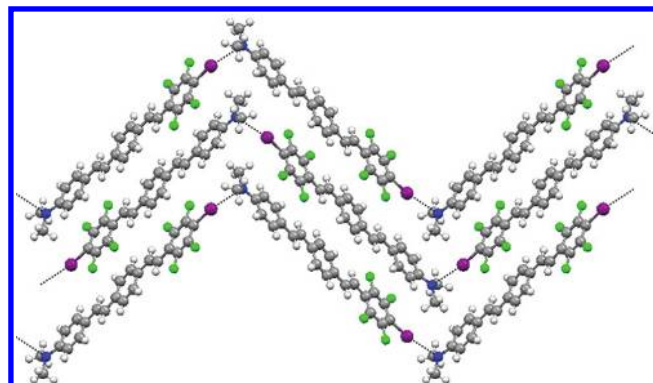

Figure 1. A ball-and-stick view down the crystallographic *a* axis of the infinite 1D halogen-bonded chains in the crystal packing of the self-complementary XB-based tecton **1**. Colors as follows: C, dark gray; H, light gray; F, green; I, purple; N, blue; XB, dotted black lines.

shifter. All experimental EFISH β_λ values are defined according to the "phenomenological" convention.[11]

Computational Details. The molecular structures of all the examined compounds have been optimized in $CHCl_3$ within the DFT approach, using the Gaussian suite of programs.[12] The PBE0 functional,[13,14] which has been judged well suited for describing the electronic and optical features of a series of organic dyes,[15] was used throughout for DFT calculations. The 6-311++G** basis set was chosen for all atoms. The basis set for iodine[16] was downloaded from the Basis Set Exchange site.[17] The solvation effects have been included by means of the polarizable continuum model (PCM).[18] To determine the absorption wavelengths, standard vertical time-dependent DFT (TDDFT) calculations[19−21] have been carried out with Gaussian at the PBE0/6-311++G** level, using the so-called nonequilibrium approach. Calculations of hyperpolarizability have been performed with ADF2009[22] at the same frequency as used in the experiment, using the SAOP exchange-correlation potential,[23,24] having the asymptotically correct behavior as required for NLO properties calculations[24] and the triple-ζ polarized Slater-type orbital "TZP" basis set for all atoms.

■ RESULTS AND DISCUSSION

The family of the self-complementary XB-based tectons **1−3** was designed in analogy with most of the molecular chromophores for NLO applications and consist of a push−pull system where a conjugated moiety spaces an electron-donor end, working as XB-acceptor terminus, and an electron-acceptor end, working as XB-donor terminus.[25] *N,N*-Dimethylanilino and pyridyl moieties were used as XB-acceptor groups (electron donors, Lewis bases), while the *p*-iodotetrafluorophenyl residue was chosen as a strong XB-donor group (electron acceptor, Lewis acid), which can be easily appended to a wide variety of carbon frameworks with high yield and regioselective

Figure 2. A ball-and-stick view down the crystallographic *a* axis of the infinite 1D halogen-bonded chains in the crystal packing of the self-complementary XB-based tecton **2**. Colors as in Figure 1.

reactions.[6h,m] Moreover, it could be expected that the electron withdrawing ability of fluorinated groups along with high polarizability of iodine atom both contribute to enhance a second-order NLO response.[25,26] The compounds **1−3** were obtained in good yields through standard synthetic procedures and fully characterized (see Supporting Information).

Single crystals of the push−pull systems **1−3** have been obtained upon slow evaporation at room temperature of their chloroform solutions. The single crystal X-ray analysis of those crystals gave details about the supramolecular organization of the self-complementary modules **1−3** in the crystal lattices. Both **1** and **2** crystallize in the monoclinic space group $P2_1/n$ and are isostructural (Figures 1 and 2). In particular, in both of the structures the molecules are almost planar with the tetrafluoroaromatic rings locked in the plane of the double bonds by two short intramolecular H···F hydrogen bonds in the range 2.2−2.4 Å. The amine group shows a significant planarization: the distance of the N atom from the plane of its three-bonded C atoms is 0.189(4) and 0.184(17) Å for **1** and **2**, respectively, just about at the minimum of the bimodal distribution of *N,N*-dimethylaminobenzene derivatives found in the CCDC (see Supporting Information, Figure S2). As far as the supramolecular organization of the different modules **1** and **2** in the crystal packing is concerned, they are arranged in a head-to-tail fashion forming one-dimensional (1D) unlimited chains, as it is expected for telechelic self-complementary XB-based tectons.[27] The N···I distances are 3.138(3) Å and 3.089(13) Å, in **1** and **2**, respectively, which roughly correspond to a 11% and 13% shortening of the sum of van der Waals radii for N and I (3.53 Å),[28] respectively. The N···I−C angles are 170.12(9)° (**1**) and 170.0(5)° (**2**), in good agreement with the high
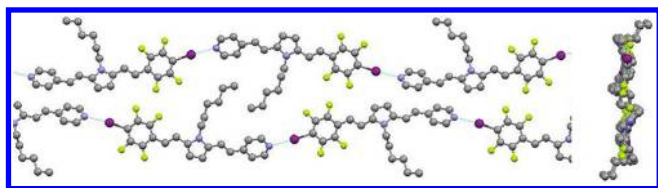
Figure 3. Left: Ball-and-stick view of a couple of infinite 1D halogen-bonded chains of the self-complementary XB-based tecton **3**. The antinodes of the stationary wave host the two hexyl chains. Right: View on the left after 90° rotation to show the flat arrangement of the couple of infinite chains.

Table 2. EFISH $\mu\beta_\lambda$ ($\times 10^{-48}$ esu) and UV–vis Absorption Maxima Measured for the Compounds 1–3 in CHCl$_3$ and DMF Solutions

compound	CHCl$_3$		DMF	
	$\mu\beta_\lambda$	λ_{max}	$\mu\beta_\lambda$	λ_{max}
1	+192	406	−465	410
2	+700	410	−2000	415
3	+220	423	−1500	425

directionality of XB and the marked n → σ* character of the electron donation from the N to I atoms.[5] The C_{Ar}–N···I angle [95.6(2)° (**1**) and 97.3(9)° (**2**)] affects the supramolecular organization of the self-complementary XB-based tectons **1** and **2** in the packing, wherein they are arranged into zigzag halogen-bonded 1D infinite chains (Figures 1 and 2). An antiparallel arrangement of the polar chains in the crystal is firmly indicated by the centric space group ($P2_1/n$).

The NLO-phore **3** crystallizes in the monoclinic space group $P2_1/c$. The N···I distance is 2.808(5) Å, quite shorter than in **1** and **2**, and the N···I–C angle is 169.16(11)°. Also here the perfluorinated benzene ring and its bonded ethylene group form a flat synthon, favored by the presence of two short intramolecular H···F interactions of about 2.3 Å. On the other hand, the whole conjugated molecular system is quite helicoidally distorted, the angle between the mean planes through the terminal aromatic rings being 36.9(2)°. Because of this torsion, antiparallel unlimited polymeric chains are coupled forming a sort of stationary wave (Figure 3, left). The antinodes host the hexyl chains having a *gtt* conformation, so that the two chains system is quite flat (Figure 3, right). The halogen bond being the only strong interaction in the crystal, the overall packing is due essentially to residual forces and there are only two attractive H···F intermolecular distances of about 2.60 Å, scarcely below the sum of van der Waals radii for H and F.[28]

The lack of polarity in the crystalline structures of **1**–**3** can be easily explained taking into account previous reports by Glaser et al.[29] Studies of point dipole lattice have shown in fact that the antiparallel alignment of polar molecules is always preferred over the parallel one, since electrostatic forces tend to align polar molecules such that molecular dipoles are canceled. The presence of a high molecular dipole moment in compounds **1**–**3** leads to a centrosymmetric crystal packing, and their solid-state utilization as prospect NLO materials would require the use of poling strategies in order to achieve a permanent polar order of the self-assembled 1D infinite chains formed through XB.[30,31]

In order to characterize their electro-optic behavior at the molecular level, we decided to undertake a detailed study of the second-order NLO properties of the compounds **1**–**3** by the solution-phase electric field induced second-harmonic (EFISH) generation method.[8–10] The measurements of $\mu\beta_\lambda$, the product of the molecular dipole moment and the projection of β_{tot}, the "vectorial part" of the quadratic hyperpolarizability tensor, along μ, of the chromophores **1**–**3** were first carried out in CHCl$_3$ solutions at 1907 nm nonresonant wavelength. The obtained $\mu\beta_\lambda$ values were all positive (see Table 2), and in the case of **1** and **3** very close to those measured for closely related structures (e.g., the pentafluoro analogue of **1** showed $\mu\beta_\lambda$ values of +200 × 10^{48} esu).[25a] Differently, besides being positive, **2** shows a very

high $\mu\beta_\lambda$ value. Such an unexpected large increase of the $\mu\beta_\lambda$ going from **1** to **2** has been confirmed by DFT PBE0/6-311++G** and TDDFT SAOP/TZP calculations in chloroform (see Table 3).

The series of compounds with one, two, and three double bonds bridging the terminal aromatic groups (**4**, **1**, and **5**, respectively) has been studied, besides compound **2**, in order to evaluate the role of the phenyl ring vs double bond spacer in modulating the second-order NLO response of the examined chromophores. The computed $\mu\beta_\lambda$ value for the compound **2** amounts to 3.45 times that of compound **1**, in good agreement with the 3.65 increasing ratio observed experimentally (see Table 2). On the other hand, the corresponding ratio for compounds with three vs two double bonds (i.e., **5** vs **1**) is 1.43, denoting a more effective and steeply increasing contribution to the NLO response of the chromophores **1**–**5** of the phenyl ring compared to the double bond.

A possible explanation of such results can be given by resorting to the phenomenological Oudar two-level model,[32] giving the charge-transfer (CT) contribution to the quadratic hyperpolarizability, $\beta_{CT} \propto (\mu^2_{eg}\Delta\mu_{eg}/\Delta E^2_{eg})$, wherein μ_{eg} is the transition dipole moment, $\Delta\mu_{eg}$ is the difference between the dipole moment of the excited and ground states, and ΔE_{eg} is the excitation energy. The UV–vis absorption spectra in CHCl$_3$ show one major band at 406 and 410 nm, for **1** and **2**, respectively (see Table 2). This band can be attributed to the intramolecular CT transition to the lowest energy excited state emanating from the NMe$_2$ donor-end of the molecule. The assignment of the UV major band has been confirmed by TDDFT PBE0/6-311++G** calculations in chloroform on compounds **1**, **2**, besides the model compounds **4** and **5** (see Table 3). Calculations predicted for all compounds one major band, corresponding to the HOMO → LUMO transition, placed at a higher wavelength than the experimental one, but within the 100 nm maximum deviation provided by the PBE0 functional for a series of organic dyes.[15a] The HOMO and LUMO were both π orbitals, the former principally localized on the donor moiety and the π bridge of the molecule, and the latter on the acceptor moiety and the π bridge of the molecule (see Figure S1 in Supporting Information for a HOMO–LUMO plot of the compound **2**). This transition is therefore associated with an increase $\Delta\mu_{eg}$ of the dipole moment from the ground (μ_g) to the excited state (μ_e). Data reported in Table 3 show that, while μ_g is comparable for all the examined compounds, μ_e undergoes a moderate increase with an increase in the number of conjugated double bonds, but shows a sudden rise for compound **2**.

The large $\Delta\mu_{eg}$ value computed for the latter compound is apparent from Figure 4, which reports a plot of the electrostatic potential for the ground and the excited states of **2**. Such results should explain, in terms of the Oudar model, the better

Table 3. Computed Ground State Dipole Moments (μ), Dynamic Hyperpolarizabilities (β_{dyn}), and Electronic Transitions (λ_{max}) of Compounds 1, 2, and the Model Compounds 4 and 5, along with the Associated Excited State Dipole Moments (μ_e), the Transition Dipole Moments (μ_{eg}), and the Oscillator Strengths (f)[a]

compound	μ (D)	λ_{max} (nm)	f	μ_{eg} (D)	μ_e (D)	β_{dyn} ($\times 10^{-30}$ esu)	$\mu\beta_\lambda{}^b$ ($\times 10^{-48}$ esu)
1	7.60	401	1.45	11.1	19.5	71	542
2	8.30	483	1.80	13.6	31.5	605	5017
4	8.95	444	1.89	13.3	22.9	163	1454
5	9.66	482	2.28	15.3	25.1	225	2073

[a] Ground state properties and electronic transitions computed at DFT PBE0/6-311++G** level with Gaussian09. Hyperpolarizabilities computed at DFT SAOP/TZP level with ADF2009. [b] β_λ computed as $(\mu \cdot \beta_{dyn})/|\mu|$.
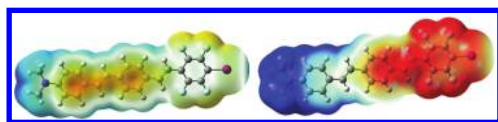
Figure 4. Plots of the electrostatic potential of compound **2** in the ground (left) and the excited state corresponding to the major band (right). Potentials are mapped on the respective isosurfaces (0.0004 au) of electron density. Values of electrostatic potential range from −0.04 (red) to 0.04 (blue) a.u. Atom color scheme: C, gray; H, light gray; N, dark blue; F, sky blue, I, magenta.

performance of compound **2** with respect to push—pull compounds whose π bridge is uniquely constituted by double bonds. It has, however, to be noted, as previously observed by other authors,[33] that an optimal performance is obtained with an alternation of phenyl rings and double bonds along the π bridge. In fact, a sequence of only aromatic rings is detrimental for the NLO response owing to the loss of planarity of the chromophore deriving from sterical hindrance.[34]

It is well established, both experimentally and theoretically, that the environment strongly influences NLO responses of molecules.[35] In fact, there are many examples of theoretical and experimental investigations describing that the formation of specific solute—solvent HB increases the value of β. Similarly, we have already demonstrated that the occurrence of XB influences the NLO properties of molecules in solution.[7a] Here we have extended a similar study to the new NLO chromophores **2** and **3** whose EFISH $\mu\beta_\lambda$ values measured in CHCl$_3$ and DMF solutions are reported in Table 2 together with UV—vis absorption maxima. Interestingly, in agreement with what was previously observed for **1**, an inversion, from positive to negative, of the sign of the $\mu\beta_\lambda$ values is also observed for **2** and **3** on going from CHCl$_3$ to DMF. Theoretical studies are consistent with the rationalization that the solvent dependence of the sign of the $\mu\beta_\lambda$ value is related to the involvement of the I atom of **1**—**3** in the formation of specific halogen-bonded adducts where the XB-acceptor is DMF. Noticeably, the absolute value of $\mu\beta_\lambda$ is the greatest for the NLO-phore **2** also in DMF.

■ CONCLUSIONS

In conclusion, we have described the synthesis of the self-complementary, XB-based push—pull molecules **1**—**3** and their single crystal X-ray structures have been reported. The molecular structures of these tectons were designed in order to show optical nonlinearities and possess self-complementary XB-donor and acceptor groups driving their self-assembly into head-to-tail halogen-bonded infinite polar chains. However, such polar chains aggregate according to a centrosymmetric crystal structure

giving macroscopically a null second-order NLO response. The design was then optimized by varying the π bridge of the push—pull molecules introducing double bonds, aromatic rings, and combination thereof, in order to maximize NLO responses. Theoretical calculations supported the design of the new NLO-phores **1**—**3**, and allowed the high hyperpolarizabilities observed in solution to be rationalized.

It is now widely accepted that organic materials might be valuable for use in certain NLO applications.[25] Considering the easy introduction of the iodotetrafluorophenyl residue on any molecular scaffolds, and the effectiveness of XB in driving the formation of infinite polar chains, the design principle described in this paper may guide the preparation of new powerful NLO organic materials, provided optimized molecular frameworks are chosen and either formation of centrosymmetric crystals is avoided or effective poling strategies are used.

■ ASSOCIATED CONTENT

ⓢ Supporting Information. Experimental details, NMR, ESI-MS, and IR studies of the complex in the solid state, computational and crystallographic details. This material is available free of charge via the Internet at http://pubs.acs.org.

■ AUTHOR INFORMATION

Corresponding Author
*(E.C.) Phone: +39 02 50314370. Fax: +39 02 50314405. E-mail: elena.cariati@unimi.it. (A.F.) Phone: +39 02 50314273. Fax: +39 02 50314300. E-mail: alessandra.forni@istm.cnr.it. (P.M, G.R.) Phone: +39 02 23993041 (P.M.), +39 02 23993032 (G.R.). Fax: +39 02 23993180. E-mail: pierangelo.metrangolo@polimi.it (P.M.), giuseppe.resnati@polimi.it (G. R.).

■ ACKNOWLEDGMENT

■ REFERENCES

(1) Selected references: (a) Schreiner, P. R. *Chem. Soc. Rev.* **2003**, 32, 289–296. (b) Choi, K.; Hamilton, A. D. *Coord. Chem. Rev.* **2003**,

5646

dx.doi.org/10.1021/cg201194a |*Cryst. Growth Des.* 2011, 11, 5642–5648

240, 101–110. (c) Custelcean, R. *Chem. Commun.* **2008**, 295–307. (d) Datta, A.; Pati, S. K. *Chem. Soc. Rev.* **2006**, *35*, 1305–1323. (e) Yagai, S. *J. Photochem. Photobiol. C: Photochem. Rev.* **2006**, *7*, 164–182. (f) Maity, S.; Guin, M.; Singh, P. C.; Patwari, G. N. *ChemPhysChem* **2011**, *12*, 26–46. (g) Lehn, J.-M. *Science* **2002**, *295*, 2400–2403. (h) Corbin, P. S.; Zimmerman, S. C.; Thiessen, P. A.; Hawryluk, N. A.; Murray, T. J. *J. Am. Chem. Soc.* **2001**, *123*, 10475–10488. (i) Whitesides, G. M.; Mathias, J. P.; Seto, C. T. *Science* **1991**, *254*, 1312–1319.

(2) (a) Polishak, B. M.; Huang, S.; Luo, J.; Shi, Z.; Zhou, X.-H.; Hsu, A.; Jen, A.K.-Y. *Macromolecules* **2011**, *44*, 1261–1265. (b) Bassani, D. M.; Jonusauskaite, L.; Lavie-Cambot, A.; McClenaghan, N. D.; Pozzo, J.-L.; Ray, D.; Vives, G. *Coord. Chem. Rev.* **2010**, *254*, 2429–2445. (c) Frattarelli, D.; Schiavo, M.; Facchetti, A.; Ratner, M. A.; Marks, T. J. *J. Am. Chem. Soc.* **2009**, *131*, 12595–12612. (d) DiBenedetto, S. A.; Frattarelli, D.; Schiavo, M.; Facchetti, A.; Ratner, M. A.; Marks, T. J. *J. Am. Chem. Soc.* **2009**, *131*, 11080–11090. (e) Rajesh, K.; Chandra, M. S.; Hirakawa, S.; Kawamata, J.; Radhakrishnan, T. P. *Langmuir* **2007**, *23*, 8560–8568. (f) Priimagi, A.; Cattaneo, S.; Ras, R. H. A.; Valkama, S.; Ikkala, O.; Kauranen, M. *Chem. Mater.* **2005**, *17*, 5798–5802.

(3) (a) Kippelen, B. *Nat. Mater.* **2004**, *3*, 841–843. (b) Zou, G.; Wang, Y.; Zhang, Q.; Kohn, H.; Manaka, T.; Iwamoto, M. *Polymer* **2010**, *51*, 2229–2235. (c) You, X.; Chen, X.; Zou, G.; Su, W.; Zhang, Q.; He, P. *Chem. Phys. Let.* **2009**, *482*, 129–133. (d) Ye, Q.; You, X.; Zou, G.; Yu, X.; Zhang, Q. *J. Mater. Chem.* **2008**, *18*, 2775–2780.

(4) (a) Macchi, R.; Cariati, E.; Marinotto, D.; Tordin, E.; Ugo, R.; Santoro, G.; Ubaldi, M. C.; Pietralunga, S. M.; Mattei, G. *J. Mater. Chem.* **2011**, *21*, 9778–9783. (b) Cabanetos, C.; Blart, E.; Pellegrin, Y.; Montembault, V.; Fontaine, L.; Adamietz, F.; Rodriguez, V.; Odobel, V., F. *Polymer* **2011**, *52*, 2286–2294. (c) Zhou, X.-H.; Luo, J.; Huang, S.; Kim, T.-D.; Shi, Z.; Cheng, Y.-J.; Jang, S.-H.; Knorr, D. B., Jr.; Overney, R. M.; Jen, A.K.-Y. *Adv. Mater.* **2009**, *21*, 1976–1981. (d) Ma, X.; Liang, R.; Yang, F.; Zhao, Z.; Zhang, A.; Song, N.; Zhou, Q.; Zhang, J. *J. Mater. Chem.* **2008**, *18*, 1756–1764. (e) Facchetti, A.; Annoni, E.; Beverina, L.; Morone, M.; Zhu, P.; Marks, T.; Pagani, G. *Nat. Mater.* **2004**, *3*, 910–917.

(5) (a) Caballero, A.; White, N. G.; Beer, P. D. *Angew. Chem., Int. Ed.* **2011**, *50*, 1845–1848. (b) Politzer, P.; Murray, J. S.; Clark, T. *Phys. Chem. Chem. Phys.* **2010**, *12*, 7748–7757. (c) Casnati, A.; Cavallo, G.; Metrangolo, P.; Resnati, G.; Ugozzoli, F.; Ungaro, R. *Chem.—Eur. J.* **2009**, *15*, 7903–7912. (d) Raatikainen, K.; Huuskonen, J.; Lahtinen, M.; Metrangolo, P.; Rissanen, K. *Chem. Commun.* **2009**, 2160–2162. (e) Metrangolo, P.; Meyer, F.; Pilati, T.; Resnati, G.; Terraneo, G. *Angew. Chem., Int. Ed.* **2008**, *47*, 6114–6127. (f) Sun, A.; Lauher, J. W.; Goroff, N. S. *Science* **2006**, *312*, 1030–1034. (g) Metrangolo, P.; Neukirch, H.; Pilati, T.; Resnati, G. *Acc. Chem. Res.* **2005**, *38*, 386–395. (h) Metrangolo, P.; Resnati, G. *Chem.—Eur. J.* **2001**, *7*, 2511–2519. (i) Corradi, E.; Meille, S. V.; Messina, M. T.; Metrangolo, P.; Resnati, G. *Angew. Chem.* **2000**, *112*, 1852–1856. *Angew. Chem., Int. Ed.* **2000**, *39*, 1782–1786.

(6) (a) Bolton, O.; Lee, K.; Kim, H. J.; Lin, K. Y.; Kim, J. *Nature Chem.* **2011**, *3*, 205–210. (b) Lemouchi, C.; Vogelsberg, C. S.; Zorina, L.; Simonov, S.; Batail, P.; Brown, S.; Garcia-Garibay, M. A. *J. Am. Chem. Soc.* **2011**, *133*, 6371–6379. (c) Bruce, D. W.; Metrangolo, P.; Meyer, F.; Pilati, T.; Präsang, C.; Resnati, G.; Terraneo, G; Wainwright, S. G.; Whitwood, A. C. *Chem.—Eur. J.* **2010**, *16*, 9511–9524. (d) Metrangolo, P.; Carcenac, Y.; Lahtinen, M.; Pilati, T.; Rissanen, K.; Vij, A.; Resnati, G. *Science* **2009**, *323*, 1461–1464. (e) Casnati, A.; Liantonio, R.; Metrangolo, P.; Resnati, G.; Ungaro, R.; Ugozzoli, F. *Angew. Chem.* **2006**, *118*, 1949–1952. *Angew. Chem., Int. Ed.* **2006**, *45*, 1915–1918. (f) Mele, A.; Metrangolo, P.; Neukirch, H.; Pilati, T.; Resnati, G. *J. Am. Chem. Soc.* **2005**, *127*, 14972–14973. (g) Xu, J.; Liu, X.; Lin, T.; Huang, J.; He, C. *Macromolecules* **2005**, *38*, 3554–3557. (h) Auffinger, P.; Hays, F. A.; Westhof, E.; Ho, P. S. *Proc. Natl. Acad. Sci. U. S. A.* **2005**, *102*, 7157–7162. (i) Caronna, T.; Liantonio, R.; Logothetis, T. A.; Metrangolo, P.; Pilati, T.; Resnati, G. *J. Am. Chem. Soc.* **2004**, *126*, 4500–4501. (j) Fourmigue, M.; Batail, P. *Chem. Rev.* **2004**, *104*, 5379–5418. (k) Nguyen, H. L.; Horton, P. N.; Hursthouse, M. B.; Legon, A. C.; Bruce, D. W. *J. Am. Chem. Soc.* **2004**, *126*, 16–17. (l) Bertani, R.; Metrangolo, P.; Moiana, A.; Perez, E.; Pilati, T.; Resnati, G.; Rico-Lattes, I.; Sassi, A. *Adv. Mater.* **2002**,

14, 1197–1201. (m) Farina, A.; Meille, S. V.; Messina, M. T.; Metrangolo, P.; Resnati, G.; Vecchio, G. *Angew. Chem.* **1999**, *111*, 2585–2588. *Angew. Chem., Int. Ed.* **1999**, *38*, 2433–2436.

(7) (a) Cariati, E.; Forni, A.; Biella, S.; Metrangolo, P.; Meyer, F.; Resnati, G.; Righetto, S.; Tordin, E.; Ugo, R. *Chem. Commun.* **2007**, 2590–2592. (b) Marras, G.; Metrangolo, P; Meyer, F; Pilati, T.; Resnati, G.; Vij, A. *New J. Chem.* **2006**, *30*, 1397. (c) Thallapally, P. K.; Desiraju, G. R.; Bagieu-Beucher, M.; Masse, R.; Bourgogne, C.; Nicoud, J. F. *Chem. Commun.* **2002**, 1052–1053. (d) Bond, A. D.; Griffiths, J.; Rawson, J. M.; Hulliger, J. *Chem. Commun.* **2001**, 2488–2489. (e) Jagarlapudi, A. R. P. S.; Allen, F. H.; Hoy, V. J.; Howard, J. A. K.; Thaimattam, R.; Biradha, K.; Desiraju, G. R. *Chem. Commun.* **1997**, 101–102.

(8) Singer, K. D.; Garito, A. F. *J. Chem. Phys.* **1981**, *75*, 3572–3580.

(9) Levine, B. F.; Bethea, C. G. *Appl. Phys. Lett.* **1974**, *24*, 445–447.

(10) Ledoux, I.; Zyss, J. *Chem. Phys.* **1982**, *73*, 203–213.

(11) Willetts, A.; Rice, J. E.; Burland, D. M.; Shelton, D. P. *J. Chem. Phys.* **1992**, *97*, 7590–7599.

(12) Frisch, M. J. et al. *Gaussian 09*, Revision A.2; Gaussian, Inc.: Wallingford CT, 2009.

(13) Ernzerhof, M.; Scuseria, G. E. *J. Chem. Phys.* **1999**, *110*, 5029–5036.

(14) Adamo, C.; Barone, V. *J. Chem. Phys.* **1999**, *110*, 6158–6170.

(15) (a) Jacquemin, D.; Perpète, E. A.; Scuseria, G. E.; Ciofini, I.; Adamo, C. *J. Chem. Theory Comput.* **2008**, *4*, 123–135. (b) Jacquemin, D.; Wathelet, V.; Perpète, E. A.; Adamo, C. *J. Chem. Theory Comput.* **2009**, *5*, 2420.

(16) Glukhovstev, M. N; Pross, A.; McGrath, M. P.; Radom, L. *J. Chem. Phys.* **1995**, *103*, 1878–1885.

(17) (a) Feller, D. *J. Comput. Chem.* **1996**, *17*, 1571–1586. (b) Schuchardt, K. L.; Didier, B. T.; Elsethagen, T.; Sun, L.; Gurumoorthi, V.; Chase, J.; Li, J.; Windus, T. L. *J. Chem. Inf. Model* **2007**, *47*, 1045–1052.

(18) Cossi, M.; Barone, V. *J. Chem. Phys.* **2001**, *115*, 4708–4717.

(19) Runge, E.; Gross, E. K. U. *Phys. Rev. Lett.* **1984**, *52*, 997–1000.

(20) Stratmann, R. E.; Scuseria, G. E.; Frisch, M. J. *J. Chem. Phys.* **1998**, *109*, 8218–8224.

(21) Casida, M. E. *J. Mol. Struct. (THEOCHEM)* **2009**, *914*, 3–18.

(22) *ADF2009, SCM, Theoretical Chemistry*; Vrije Universiteit: Amsterdam, The Netherlands, http://www.scm.com.

(23) Gritsenko, O. V.; Schipper, P. R. T.; Baerends, E. J. *Chem. Phys. Lett.* **1999**, *302*, 199–207.

(24) Schipper, P.R.T.; Gritsenko, O. V.; van Gisbergen, S. J. A.; Baerends, E. J. *J. Chem. Phys.* **2000**, *112*, 1344–1352.

(25) Papagni, A.; Maiorana, S.; Del Buttero, P.; Perdicchia, D.; Cariati, F.; Cariati, E.; Marcolli, W. *Eur. J. Org. Chem.* **2002**, 1380–1384.

(26) Romaniello, P.; Lelj, F. *J. Fluorine Chem.* **2004**, *125*, 145–149.

(27) Lucassen, A. C. B.; Vartanian, M.; Leitus, G.; van der Boom, M. E. *Cryst. Growth Des.* **2005**, *5*, 1671–1673.

(28) (a) Bondi, A. *J. Phys. Chem.* **1964**, *68*, 441–451. (b) Shannon, R. D. *Acta Crystallogr.* **1976**, *A32*, 751–767.

(29) (a) Steiger, D.; Ahlbrandt, C.; Glaser, R. *J. Phys. Chem. B* **1998**, *102*, 4257–4260. (b) Steiger, D.; Glaser, R. *J. Comput. Chem.* **2001**, *22*, 208–215. Glaser, R.; Knotts, N.; Yu, P.; Li, L.; Chandrasekhar, M.; Martin, C.; Barnes, C. L. *Dalton Trans.* **2006**, 2891–2899.

(30) Glaser, R.; Knotts, N.; Wu, H. *ChemTracts Org. Chem.* **2003**, *16*, 643–652.*Anisotropic Organic Materials-Approaches to Polar Order*; *ACS Symposium Series 798*; Glaser, R.; Kaszynski, P., Eds.; American Chemical Society: Washington, DC, 2001.

(31) (a) Gopalan, P.; Katz, H. E.; McGee, D. J.; Erben, C.; Zielinski, T.; Bousquet, D.; Muller, D.; Grazul, J.; Olsson, Y. *J. Am. Chem. Soc.* **2004**, *126*, 1741–1747. (b) Traber, B.; Wolff, J. J.; Rominger, F.; Oeser, T.; Gleiter, R.; Goebel, M.; Wortmann, R. *Chem.—Eur. J.* **2004**, *10*, 1227–1238. (c) Staub, K.; Levina, G. A.; Barlow, S.; Kowalczyk, T. C.; Lackritz, H. S.; Barzoukas, M.; Fort, A.; Marder, S. R. *J. Mater. Chem.* **2003**, *13*, 825–833. (d) Yang, M.; Champagne, B. *J. Phys. Chem. A* **2003**, *107*, 3942–3951. (e) Wolff, J. J.; Siegler, F.; Matschiner, R.; Wortmann, R. *Angew. Chem.* **2000**, *112*, 1494–1498. *Angew. Chem., Int.*

Ed. **2000**, *39*, 1436–1439. (f) Wang, F.; Harper, A. W.; Lee, M. S.; Dalton, L. R.; Zhang, H.; Chen, A.; Steier, W. H.; Marder, S. R. *Chem. Mater.* **1999**, *11*, 2285–2288. (g) Marder, S. R.; Kippelen, B.; Jen, A.K. -Y.; Peyghambarian, N. *Nature* **1997**, *388*, 845–851.

(32) Oudar, J. L.; Chemla, D. S. *J. Chem. Phys.* **1977**, *66*, 2664–2668.

(33) (a) Davis, W. B.; Wasielewski, M. R.; Ratner, M. A. *Int. J. Quantum Chem.* **1999**, *72*, 463–471. (b) Meier, H.; Gerold, J.; Kolshorn, H.; Baumann, W.; Bletz, M. *Angew. Chem., Int. Ed.* **2002**, *41*, 292–295. (c) Coe, B. J.; Harries, J. L.; Harris, J. A.; Brunschwig, B. S.; Horton, P. N.; Husthouse, M. B. *Inorg. Chem.* **2006**, *45*, 11019–11029.

(34) Cheng, L.-T.; Tam, W.; Marder, S. R.; Stiegman, A. E.; Rikken, G.; Spangler, C. W. *J. Phys. Chem.* **1991**, *95*, 10643–10652.

(35) (a) Huyskens, F. L.; Huyskens, P. L.; Persoons, A. P. *J. Chem. Phys.* **1998**, *108*, 8161–8171. (b) Abbotto, A.; Beverina, L.; Bradamante, S.; Facchetti, A.; Klein, C.; Pagani, G. A.; Redi-Abshiro, M.; Wortmann, R. *Chem.—Eur. J.* **2003**, *9*, 1991–2007 and references therein.

5648

dx.doi.org/10.1021/cg201194a |*Cryst. Growth Des.* 2011, 11, 5642–5648